Reactions of $Fe(CO)_4$ with C_2H_5I in the Gas Phase: Evidence for the Formation of $IFe(CO)_4(C_2H_5)$, $IFe(CO)_3(\eta^2\text{-}COC_2H_5)$, and $IFe(CO)_4(COC_2H_5)$

David L. Cedeño*,† and Eric Weitz*,‡

Department of Chemistry, Illinois State University, Normal, Illinois 61790-4160, and Department of Chemistry, Northwestern University, Evanston, Illinois 60208-3113

Received October 4, 2004

The reaction of C_2H_5I with photogenerated $Fe(CO)_4$ was followed using time-resolved infrared spectroscopy. Three novel products were detected. On the basis of their carbonyl stretching frequencies, their kinetics, and calculations of their relative energies, these complexes are assigned as $IFe(CO)_4(C_2H_5)$, $IFe(CO)_3(\eta^2\text{-}COC_2H_5)$, and $IFe(CO)_4(COC_2H_5)$. Addition of C_2H_5I to $Fe(CO)_4$ produces $IFe(CO)_4(C_2H_5)$ as the kinetically preferred product, which then converts to $IFe(CO)_3(\eta^2\text{-}COC_2H_5)$, the thermodynamically preferred complex. $IFe(CO)_4(COC_2H_5)$ is formed upon addition of CO to $IFe(CO)_3(\eta^1\text{-}COC_2H_5)$, a 16-electron complex that is proposed as a common intermediate leading to the three products. Temperature-dependent studies of the kinetics of the decay of $IFe(CO)_4(COC_2H_5)$, the longest lived of the products, indicate that it decarbonylates with an activation energy of ∼20 kcal/mol.

I. Introduction

Of the many reactions involving organometallic compounds, oxidative addition stands out as one of the most important classes. Such reactions often involve the activation of a bond in a bound ligand that would not be activated in the unbound ligand under the same conditions. The outcome of such a chemical process, which is facilitated by a transition metal, is the possibility of carrying out novel reactions that would not otherwise be facile.[1−3]

One particularly interesting and important example of an oxidative addition reaction is the cleavage of a C−X bond in an alkyl halide to produce a metal−alkyl complex:

$$M + R{-}CH_2X \rightarrow X{-}M{-}CH_2R \qquad (1)$$

where M is an unsaturated transition metal complex that increases its formal oxidation state by two. It is well established that in metal carbonyl−alkyl complexes a "migratory insertion" reaction can take place yielding the respective acetyl complex:

$$CO{-}M{-}CH_2R \rightarrow M{-}COCH_2R \qquad (2)$$

The general aspects of the mechanism for production of acetyl complexes are relevant for the understanding of many homogeneous catalytic processes such as hydroformylation and carbonylation.[4−6]

Among the best studied systems are those involving metal carbonyl complexes of iron. Early studies by Pańkowski and Bigorgne[7] reported that $Fe(CO)_5$ did not react thermally with methyl iodide in an *n*-hexane solution. Stone and co-workers[8−10] isolated the oxidative addition product from the reaction of $Fe(CO)_5$ and some perfluroroalkyliodides, but they did not report the observation of an acetyl derivative. More recent studies by Cardaci, Reichenbach, and co-workers[11−15] have assigned species involved in the carbonylation of $IFe(CO)_2(PMe_3)_2(CH_3)$ and have performed kinetic and thermodynamic studies that led them to propose a mechanism for this reaction in solution. Ford and co-workers[16−18] have carried out extensive time-resolved studies directed toward the elucidation of the intermediates involved in "migratory insertion" processes in the $(\eta^5\text{-}C_5H_5)Fe(CO)(COCH_3)$ complex in different solvents.

† Illinois State University.
‡ Northwestern University.

(1) Collman, J. P.; Hegedus, L. S.; Norton, J. R.; Finke, R. G. *Principles and Applications of Organotransition Chemistry*; University Science Books: Mill Valley, CA, 1987.
(2) Crabtree, R. H. *The Organometallic Chemistry of Transition Metals*, 3rd ed.; Wiley: New York, 2001.
(3) Collman, J. P.; Roper, W. R. *Adv. Organomet. Chem.* **1968**, *7*, 53.
(4) Parshall, G. W.; Ittel, S. D. *Homogeneous Catalysis*; John Wiley and Sons: New York, 1992.
(5) Blackborow, J. R.; Daroda, R. J.; Wilkinson, G. *Coord. Chem. Rev.* **1982**, *43*, 17.
(6) Wojcicki, A. *Adv. Organomet. Chem.* **1973**, *11*, 87.
(7) Pańkowski, M.; Bigorgne, M. *J. Organomet. Chem.* **1971**, *30*, 227.
(8) Manuel, T. A.; Stafford, S. L.; Stone, F. G. A. *J. Am. Chem. Soc.* **1961**, *83*, 249.
(9) King, R. B.; Stafford, S. L.; Treichel, P. M.; Stone, F. G. A. *J. Am. Chem. Soc.* **1961**, *83*, 3604.
(10) Pitcher, E.; Stone, F. G. A. *Spectrochim. Acta* **1962**, *18*, 585.
(11) Bellachioma, G.; Cardaci, G.; Reichenbach, G. *J. Organomet. Chem.* **1981**, *221*, 291.
(12) Reichenbach, G.; Cardaci, G.; Bellachioma, G. *J. Chem. Soc., Dalton Trans.* **1982**, 847.
(13) Cardaci, G.; Reichenbach, G.; Bellachioma, G. *Inorg. Chem.* **1984**, *23*, 2936.
(14) Bellachioma, G.; Cardaci, G.; Jablonski, J.; Macchioni, A.; Reichenbach, G. *Inorg. Chem.* **1993**, *32*, 2404.
(15) Bellachioma, G.; Cardaci, G.; Macchioni, A.; Reichenbach, G.; Foresti, E.; Sabatino, P. *J. Organomet. Chem.* **1997**, *531*, 227.
(16) McFarlane, K. L.; Ford, P. C. *Organometallics* **1998**, *17*, 1166.
(17) McFarlane, K. L.; Lee, B.; Fu, W.; van Eldik, R.; Ford, P. C. *Organometallics* **1998**, *17*, 1826.
(18) Massick, S. M.; Ford, P. C. *Organometallics* **1999**, *18*, 4362.

10.1021/om0492348 CCC: $30.25
Publication on Web 02/17/2005

Their studies concluded that the reaction actually proceeds via alkyl migration to an adjacent carbonyl, although the nature of the intermediates is solvent dependent. For example, when the reaction is carried out in cyclohexane, either an η^2 species, in which the acetyl CO binds to the metal, or an agostic intermediate is a key species in the formation of the acetyl products. However, when the reaction is carried out in tetrahydrofuran, a solvento acetyl complex is postulated as the intermediate. An advantage of gas phase studies of oxidative addition processes and any subsequent reactions in these systems is that they preclude the involvement of solvent in the reaction pathway.

This paper reports on the reaction of ethyl iodide with photogenerated $Fe(CO)_4$ in the gas phase. Selective UV photolysis of $Fe(CO)_5$ provides a direct route to unsaturated species,[19] such as $Fe(CO)_4$, which would be expected to react with alkyl halides. Such reactions could lead to the formation of an alkyl halide iron tetracarbonyl complex, ($XFe(CO)_4(CH_2R)$), and subsequently to its acetyl derivative ($XFe(CO)_4(COCH_2R)$). Time-resolved infrared laser spectroscopy and time-resolved FTIR,[20,21] which have been successfully used to probe reaction intermediates and reaction products in analogous reactions, are used in these studies. Evidence for the formation of novel complexes that result from oxidative addition ($IFe(CO)_4(C_2H_5)$) and alkyl migration ($IFe(CO)_3(\eta^2\text{-}COC_2H_5)$ and $IFe(CO)_4(COC_2H_5)$) is presented. A general reaction mechanism is proposed in light of the available experimental evidence. This mechanism involves the formation of the intermediate $IFe(CO)_3(\eta^1\text{-}COC_2H_5)$ from $IFe(CO)_4(C_2H_5)$, which then leads to formation of $IFe(CO)_3(\eta^2\text{-}COC_2H_5)$, and $IFe(CO)_4(COC_2H_5)$ after subsequent addition of CO. Data in the literature for related systems[16−18] suggest that formation of $IFe(CO)_3(\eta^1\text{-}COC_2H_5)$ from $IFe(CO)_4(C_2H_5)$ takes place via migration of the ethyl to a neighboring CO ligand. Results from this study support that conclusion. Chemical kinetics simulations and density functional theory (DFT) calculations are used to assist in formulating and evaluating the overall mechanism.

II. Experimental Section

The experimental details of the time-resolved infrared laser spectroscopy technique that is used to study the sub-millisecond processes involved in the reaction of $Fe(CO)_4$ with C_2H_5I have been described elsewhere.[22] A brief description is provided here for convenience. Gas phase $Fe(CO)_5$ (0.020−0.100 Torr), CO (0−150 Torr), and ethyl iodide (0−40 Torr) are introduced into a 42 cm water-jacketed Pyrex glass cell terminated by CaF_2 windows. When necessary, sufficient helium was added to the photolysis cell in order to ensure that the rate measurements were performed in the "high-pressure limit".[20] Photolysis of $Fe(CO)_5$ was accomplished using the unfocused output of a XeCl excimer laser at 308 nm, operating at a pulse rate of 1 Hz, with a fluence of ~6−7 mJ/cm^2 at the cell window. Photolysis at 308 nm produces $Fe(CO)_3$ as the only observable product, which then forms $Fe(CO)_4$ upon addition of CO. To probe the kinetics of the reactants and products, the infrared beam of a tunable infrared diode laser was double passed through the cell. The IR beam from this laser was detected with a fast liquid N_2-cooled InSb detector. The output of this detector was amplified with either a Perry (x100) or SRS560 (variable gain) amplifier and sent to a digital storage oscilloscope, which collected and averaged signals from 10 to 30 laser pulses. The averaged signal was sent to a computer for further analysis. Rate constants for ligand addition reactions were obtained from the slope of a plot of the measured rate of reaction versus the ligand pressure. Time-resolved infrared spectra are constructed from individual time traces taken over a given probe laser frequency range. A computer is then used to connect a point from each transient at a common time delay, such that the spectrum at that particular time delay is generated. This procedure is then repeated for subsequent time delays to produce a set of spectra that allows the time evolution of a reacting system to be followed. Temperature control was achieved using a constant-temperature water bath, which circulated water through the cell jacket. The temperature was monitored using a calibrated chromel−alumel thermocouple with an uncertainty of ±1 K

A different experimental setup[22] was used to study the decay of the most stable product (lifetimes of seconds or more). In these experiments a mixture of $Fe(CO)_5$ (0.05−0.10 Torr), C_2H_5I (4−40 Torr), and CO (10−250 Torr) was introduced into a 42 cm glass cell terminated with CaF_2 windows. The mixture was photolyzed with the 355 nm output of a frequency-tripled Nd:YAG laser, with a fluence of ~6−7 mJ/cm^2 at the cell window. $Fe(CO)_4$ is produced as a major product at 355 nm.[19,23] The experiment is initiated by photolysis of the mixture for 20−40 s at a laser frequency of 10 Hz. The rise and decay of absorptions were monitored using an FTIR spectrometer operating in its "GC mode" over the 1900−2200 cm^{-1} frequency range. A liquid N_2-cooled InSb detector was again used to detect the infrared beam. Temperature control was achieved by using heating tape wrapped uniformly around the length of the cell. The temperature was monitored using a calibrated chromel−alumel thermocouple, with an uncertainty of ±1 K.

$Fe(CO)_5$ (Aldrich) was subjected to a freeze−pump−thaw cycle before a series of experiments to eliminate any CO produced from thermal decomposition. Ethyl iodide (>95% Aldrich) was subjected to at least three freeze−pump−thaw cycles prior to usage. CO (99.9% Matheson) and helium (99.999%, Praxair) were used as received.

III. Computational Methods

All density functional theory calculations of geometries, energies, and unscaled frequencies were performed under the same conditions as reported in ref 24, using the Jaguar computational package.[25] For convenience, these are briefly described here. The DFT method utilized is the BP86/VWN. Past studies[26,27] have demonstrated that this DFT method provides reliable geometries and energy calculations for iron carbonyl compounds. The BP86/VWN method employs the local functional by Slater[28] and the nonlocal gradient correction by Becke[29] to describe electron exchange. Electron correlation is described locally with the functional by Vosko, Wilk, and Nusair[30] and the nonlocal gradient correction by Perdew.[31] All

(19) Seder, T. A.; Ouderkirk, A. J.; Weitz, E. *J. Phys. Chem.* **1986**, *85*, 1977.
(20) Weitz, E. *J. Phys. Chem.* **1994**, *98*, 11256.
(21) Weitz, E. In *Energetics of Stable Molecules and Reactive Intermediates*; Minas de Piedade, M. E., Ed.; Kluwer Academic Publishers: Norwell, MA, 1999; p 215.
(22) Cedeño, D. L.; Weitz, E. *J. Phys. Chem. A* **2000**, *104*, 8011.
(23) Ryther, R. J.; Weitz, E. *J. Phys. Chem.* **1991**, *95*, 9841
(24) Wang, X.; Weitz, E. *J. Phys. Chem. A* **2002**, *106*, 11782.
(25) *Jaguar 4.1.*; Schrodinger Inc.: Portland, OR, 1998−1999.
(26) Cedeño, D. L.; Weitz, E. *Organometallics* **2003**, *22*, 2652.
(27) Wang, W.; Weitz, E. *J. Phys. Chem.* **1997**, *101*, 2358.
(28) Slater, J. C. *Quantum Theory of Molecules and Solids, Vol. 4: The Self-Consistent Field for Molecules and Solids*; McGraw-Hill: New York, 1974.
(29) Becke, A. D. *Phys. Rev. A* **1988**, *38*, 3098.
(30) Vosko, S. H.; Wilk, L.; Nusair, M. *Can. J. Phys.* **1980**, *58*, 1200.
(31) (a) Perdew, J. P. *Phys. Rev. B* **1986**, *33*, 8822. (b) Perdew, J. P. *Phys. Rev. B* **1986**, *34*, 7406.

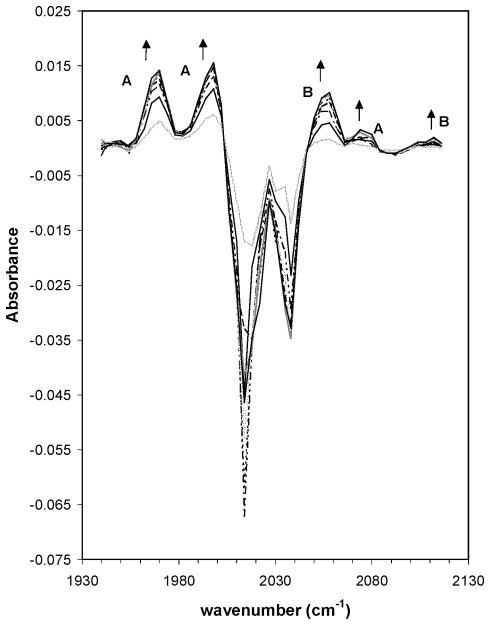

Figure 1. Time-resolved IR difference spectra obtained following 308 nm laser photolysis of 50 mTorr $Fe(CO)_5$, 10 Torr C_2H_5I, and 100 Torr CO. Spectra shown correspond to the 2−30 μs range after photolysis and are displayed every 4 μs. The "up arrows" indicate growth of products.

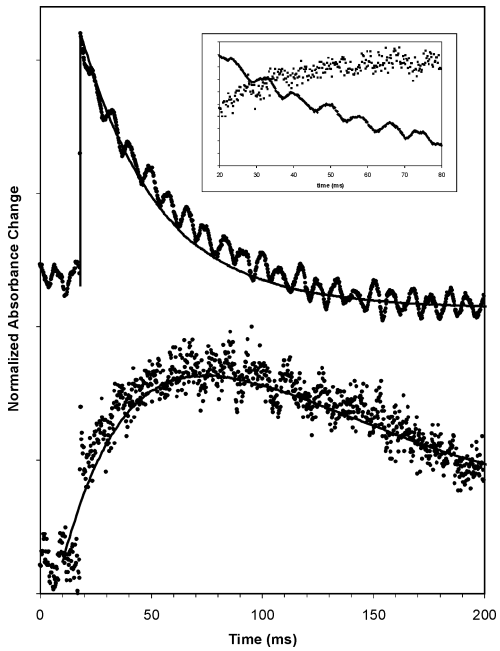

Figure 2. Transient IR signals showing the growth and decay of species A (upper trace) at 1970 cm^{-1} and growth and decay of species B (lower trace, offset for clarity) at 2058 cm^{-1}. The inset shows an enlargement of the 20−80 ms region showing that the decay of species A occurs on the same time scale as the rise of species B. See text for assignments. Lines are the results of chemical kinetics simulations; see text for details.

calculations were carried out using the LACV3P** basis set available in Jaguar 4.1. Hay and Wadt's effective core potential is used to describe the inner core electrons of iron, while a 6-31G basis set describes the core's outermost and valence electrons.[32] Nonmetal atoms are described by the 6-311G(d,p) basis set.[33] The initial guess geometries for transition state searches were obtained though a quadratic synchronous transit (QST) method between optimized product and reactants. The initial guess was then fully optimized using a linear transit method. Frequency calculations were performed on the optimized transition state to confirm it is located at a saddle point (one and only one imaginary frequency) on the potential energy surface.

IV. Results

A. Transient Spectra: μs to ms Time Scale. Figure 1 shows time-resolved spectra obtained in the 1940−2120 cm^{-1} region at 4 μs intervals from 2 to 30 μs after the 308 nm photolysis of ~0.05 Torr of $Fe(CO)_5$, 10 Torr of C_2H_5I, and 100 Torr of CO. The spectra show the appearance of products at 1970, 1998, 2058, 2072, and 2116 cm^{-1}.

Although these spectra suggest that $Fe(CO)_5$ is decaying on the same time scale as the rise of products, this apparent decay time is a result of the finite response time of the detection system. With a smaller resistance load on the detection system, which produces a faster response time (albeit poorer signal-to-noise levels), it is obvious that the decay of $Fe(CO)_5$, which is due to its photolytic depletion, occurs on a much shorter time scale than the rise of products. It was also observed that the rate of rise of products is independent of the pressure of the parent molecule, which indicates that the products are not polynuclear metal complexes formed by the addition of $Fe(CO)_5$ to an unsaturated species. The bands at 1970, 1998, and 2072 cm^{-1} have the same temporal behavior, consistent with their source being a common product. This product will be referred to as species A until a specific assignment is made.

The bands at 2058 and 2116 cm^{-1} also have a common slow rise and decay, which is consistent with their source being a common product, which will be called species B. However, the transients at 2116 cm^{-1}, while of poorer quality than those taken at 2058 cm^{-1}, do not exhibit the initial rapid rise seen in trace b in Figure 2 (note points at ~25 ms). Thus, we believe this apparent rise is a result of an overlap between the 2058 cm^{-1} absorption of species B and the 2072 cm^{-1} absorption of species A.

To determine the rate constant for addition of C_2H_5I to $Fe(CO)_4$, the rate of decay of $Fe(CO)_4$ was measured at 2001 cm^{-1} as a function of C_2H_5I pressure. A bimolecular rate constant of $(2.9 \pm 0.8) \times 10^9$ M^{-1} s^{-1} was obtained. This rate is, within experimental error, independent of temperature in the range from 281 to 308 K. The observed rate of rise of species A is dependent on the pressure of C_2H_5I and gives a rate constant of $(2.0 \pm 1.1) \times 10^9$ M^{-1} s^{-1}, which, within experimental error, matches the rate constant for decay of $Fe(CO)_4$ in the presence of C_2H_5I. This behavior is consistent with species A being a product of the reaction of $Fe(CO)_4$ and C_2H_5I:

$$Fe(CO)_4 + C_2H_5I \rightarrow A \qquad (3)$$

Species A decays on a millisecond time scale at a rate that, within experimental error, does not change as a

(32) Hay, P. J.; Wadt, W. R. *J. Chem. Phys.* **1985**, *82*, 299.
(33) (a) Clark, T.; Chandrasekhar, J.; Spitznagel G. W.; Schleyer, P. von R. *J. Comput. Chem.* **1983**, *4*, 294. (b) Frisch, M. J.; Pople, J. A.; Binkley, J. S. *J. Chem. Phys.* **1984**, *80*, 3265. (c) Krishnan, R.; Binkley, J. S.; Seeger, R.; Pople, J. A. *J. Chem. Phys.* **1980**, *72*, 650. (d) McLean, A. D.; Chandler, G. S. *J. Chem. Phys.* **1989**, *72*, 5639.

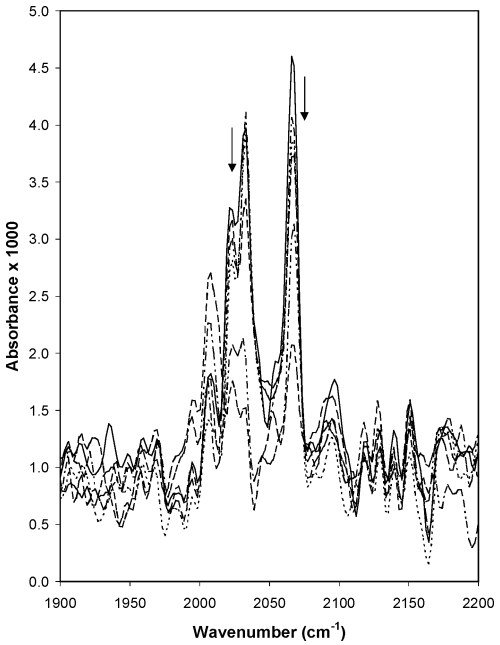

Figure 3. Time-resolved FTIR spectra obtained after 355 nm laser photolysis of 0.070 Torr $Fe(CO)_5$, 10 Torr C_2H_5I, and 106 Torr CO. The spectra shown correspond to 23, 34, 57, 108, 238, and 484 s after photolysis. A scaled spectrum of $Fe(CO)_5$ has been added to each spectrum to account for parent depletion. Down arrows indicate depletion of the species (C) being detected.

function of CO and C_2H_5I pressure. Interestingly, as apparent in Figure 2, the decay of species A takes place with a rate of 33 ± 11 s^{-1} (error limits are 2σ), that is, within experimental error, the same as the rate of rise of species B of 34 ± 12 s^{-1}. This and the independence of the rise of B on the pressures of CO, C_2H_5I, and parent are compatible with species B being a product of the decay of species A. Species B then decays via a process whose rate appears to be independent of the CO and C_2H_5I pressure. However, it was difficult to establish unequivocally that the decay of B was independent of the CO and C_2H_5I pressure given that there were lower signal-to-noise levels on the longer time scales necessary to monitor the decay of B.

B. Seconds Time Scale: Evidence for an Acetyl Product. Figure 3 shows FTIR spectra resulting from 355 nm photolysis (40 s at 10 Hz) at 297 K of a mixture containing 0.070 Torr of $Fe(CO)_5$, 10 Torr of C_2H_5I, and 106 Torr of CO. New spectral features are seen at 2008, 2022, 2033, and 2065 cm^{-1}. However, the bands at the first three frequencies are convoluted with the parent absorption, making it difficult to accurately follow their kinetics. As a result, it was possible to obtain good quality data only for the time dependence of the 2065 cm^{-1} absorption. This absorption shows a single-exponential decay whose rate is dependent on the pressure of CO present in the mixture, *decreasing* with increasing CO pressure. Such behavior suggests that CO loss is the process that leads to decay of this species (C). For a CO loss process, increasing the amount of CO present would be expected to lead to a slower decay rate. On the basis of the fact that the amount of species C that is formed is at least roughly proportional to the pressure of CO in the mixture, and that the decomposition of species C behaves similarly to that of the $IFe(CO)_2(PMe_3)_2(COCH_3)$ complex reported by Bellachioma et al.,[15] we assign species C as $IFe(CO)_4(\eta^1\text{-}COC_2H_5)$. We initially considered the possibility that C might be $Fe(CO)_4(I)_2$ because $Fe(CO)_4(I)_2$ has also been shown to decarbonylate.[34,35] However, this hypothesis was discarded because of the lack of agreement between the frequencies of the observed product and the frequencies obtained from actual samples of $Fe(CO)_4(I)_2$ that were prepared by addition of gaseous I_2 to photogenerated $Fe(CO)_4$ (see Table 1).

$IFe(CO)_4(COC_2H_5)$ may decay via a dissociative mechanism:

$$IFe(CO)_4(COC_2H_5) \rightarrow IFe(CO)_3(\eta^1\text{-}COC_2H_5) + CO \qquad k_{-CO} \quad (4)$$

$$IFe(CO)_3(\eta^1\text{-}COC_2H_5) + CO \rightarrow IFe(CO)_4(COC_2H_5) \qquad k_{CO} \quad (5)$$

$$IFe(CO)_3(\eta^1\text{-}COC_2H_5) \rightarrow \text{other products} \qquad k_{op} \quad (6)$$

If $IFe(CO)_3(\eta^1\text{-}COC_2H_5)$, which is an unsaturated 16-electron species, is present as a low concentration "steady state" intermediate on the time scale over which the decomposition takes place, then an approximate solution for the mechanism outlined in reactions 4−6 gives a phenomenological rate constant (k_{obs}) for the decay of the acetyl product, $IFe(CO)_4(COC_2H_5)$ as

$$k_{obs} = \frac{k_{-CO}k_{op}}{k_{CO}[CO] + k_{op}} \quad (7)$$

Equation 7 can be rearranged as

$$\frac{1}{k_{obs}} = \frac{1}{k_{-CO}} + \frac{k_{CO}}{k_{-CO}k_{op}}[CO] \quad (8)$$

As can be seen in Figure 4, the behavior of the dependence of k_{obs} on CO pressure is well represented by the expression in eq 7, consistent with the proposed dissociative mechanism. The rate constant for decarbonylation is then obtained from the intercept, while the ratio of the rate constant for CO addition to $IFe(CO)_3(\eta^1\text{-}COC_2H_5)$ and the phenomenological rate constant (k_{op}) for competing reactions may be obtained from the slope once k_{-CO} is determined.

C. Temperature-Dependent Studies. Figure 5 shows Arrhenius plots for the decay of species A and B. Both plots have small slopes, which are indicative of small activation energies (E_a) for the decay of species A and species B. E_a is 4.4 ± 0.9 kcal/mol for species A and 7.2 ± 1.6 kcal/mol for species B. The intercepts of these plots give the preexponetial factors (A) for the respective decay processes. The rate of decay of A is characterized by a very small preexponential: $\ln A = 10.9 \pm 1.4$. The preexponential for the decay of B is also small, with $\ln A = 14.8 \pm 2.6$. All uncertainties are based on the standard error (2σ) obtained from a linear regression fit.

Figure 6 shows an Arrhenius plot for the rate of decarbonylation (k_{-CO}) of species C. From the slope the

(34) Wojcicki, A.; Basolo, F. *J. Am. Chem. Soc.* **1961**, *83*, 525.
(35) Johnson, B. F. G.; Lewis, J.; Robinson, P. W.; Miller, J. R. *J. Chem. Soc. A* **1968**, 1043.

Table 1. Carbonyl Stretching Frequencies (in cm^{-1}) of Selected Alkyl and Acetyl Iodides

compound	experimental frequencies	calculated frequencies
$IFe(CO)_4(C_2H_5)$ [A]	2072 (w), 1998 (s), 1970 (s)[a]	2102, 2050, 2041, 2029[b]
$IFe(CO)_3(\eta^2\text{-}COC_2H_5)$ [B]	2116 (w), 2058 (s)[a]	2079, 2029, 2010, 1659[b]
$IFe(CO)_4(COC_2H_5)$ [C]	2065 (s) 2033 (?,s), 2022 (?,s)[a]	2111, 2068, 2031, 2009, 1804[a]
$IFe(CO)_3(\eta^1\text{-}COC_2H_5)$		2085, 2021, 2001, 1735[b]
$Fe(CO)_4$	2000 (s), 1984 (m)	2056, 2007, 2006, 2002[a]
$Fe(CO)_5$	2032 (s), 2018 (s)	2134, 2024, 2010, 2006[a]
$IFe(CO)_4(C_2F_5)$	2143 (m), 2112 (w), 2087 (s), 2056 (m)[c]	2052, 2050, 2036, 2031[a]
$IFe(CO)_2(PMe_3)_2(CH_3)$	1998 (vs), 1940 (s)[d]	
$IFe(CO)_2(PMe_3)_2(COCH_3)$	cis: 2018 (s), 1965 (s)[d]	
	Trans: 2044 (w), 1967 (s)[d]	
$Fe(CO)_4(I)_2$	2137 (w), 2093 (s), 2068 (m)[a]	2129, 2055, 2043, 2025[a]

[a] This work, gas phase. [b] Reference 24. [c] Reference 10, in C_2Cl_4 solution. [d] Reference 15, in *n*-hexane solution.

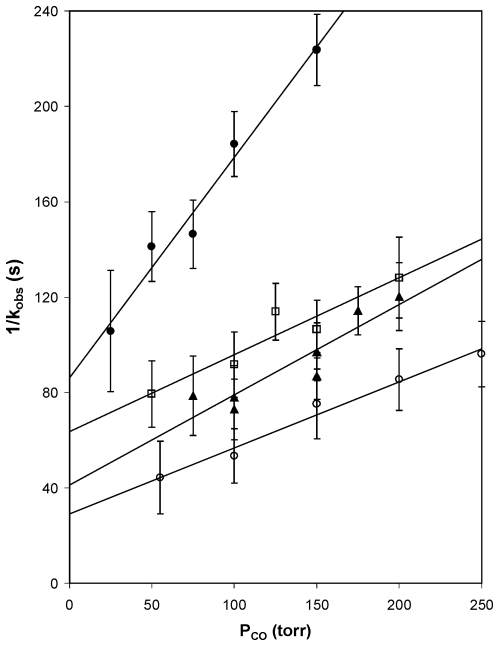

Figure 4. Plot of the inverse of the rate of decomposition ($1/k_{obs}$) of $IFe(CO)_4(COC_2H_5)$ (species C) vs CO pressure: (●) 297 K; (□) 300 K; (▲) 303 K; (○) 308 K. The intercepts correspond to $1/k_{-CO}$.

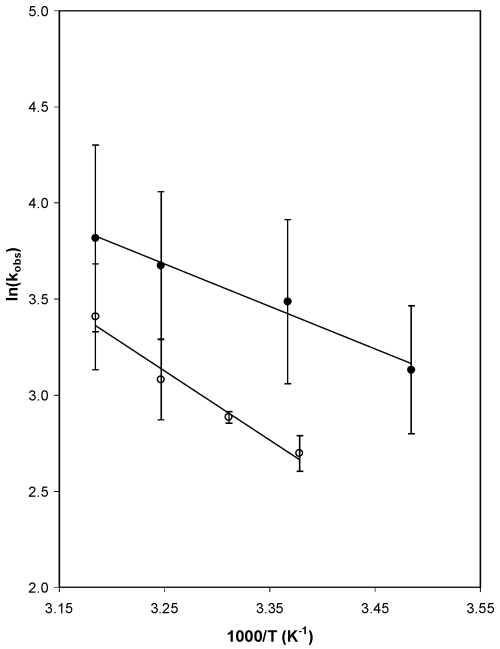

Figure 5. Arrhenius plots for the rates of decay of (●) $IFe(CO)_4(C_2H_5)$ and (○) $IFe(CO)_3(\eta^2\text{-}COC_2H_5)$. Error bars correspond to the standard deviation (2σ) of at least 8 determinations at each temperature.

energy of activation for decarbonylation is 19.6 ± 4.9 kcal/mol, and from the intercept ln *A* is equal to 28.7 ± 8.1. The ratio of k_{CO}/k_{op} seems to be temperature independent, although this ratio has a relatively large uncertainty associated with it.

V. Discussion

A. Assignments. 1. Species C. Species C is assigned as $IFe(CO)_4(COC_2H_5)$ based on a number of factors. The relatively long lifetime of species C suggests it is a coordinatively saturated species. The fact that species C is observed only when relatively high CO pressures are present in the reaction cell is consistent with its formation from an intermediate that must add CO. Additionally, the fact that the lifetime of this species *increases* with increasing CO pressure suggests that it decays by CO loss. This is the same behavior observed for an analogous compound, $IFe(CO)_2(PMe_3)_2(COCH_3)$, which was studied in ref 15. Both $IFe(CO)_2(PMe_3)_2(COCH_3)$ and $IFe(CO)_4(COC_2H_5)$ also exhibit similar kinetic parameters for decarbonylation. Finally, consistent with the assignment of species C as a fully carbonylated acetyl complex, since the addition of ligands to unsaturated complexes have typically been found to be unactivated,[20,21] the ~20 kcal/mol activation energy (E_a) for loss of CO suggests this complex is significantly lower in energy than its precursor. The possible precursors for this species are discussed below, all of which are calculated to be of a similar but a higher energy than $IFe(CO)_4(COC_2H_5)$.[24]

We note that, as discussed in Section IV.B, we could accurately monitor the time dependence of only one of the four bands observed in Figure 3. Thus, we could not determine whether all of the bands have a common time dependence, as would be expected for a single product. Therefore, we cannot rule out multiple products. However, as indicated in Table 1, $IFe(CO)_4(COC_2H_5)$ is calculated to have four absorption bands in this spectral region, and thus there is no indication that there are any observable products on the time scale of seconds other than $IFe(CO)_4(COC_2H_5)$.

2. Species A and B. Clearly, species A is a product of the reaction between $Fe(CO)_4$ and C_2H_5I. There are a number of obvious possibilities for this complex including an $Fe(CO)_4(C_2H_5I)$ adduct, in which the alkyl halide is bound to $Fe(CO)_4$ via the C−I bond. Other alternatives are that species A is the oxidative addition product, $IFe(CO)_4(C_2H_5)$, or that it is an η^1 or η^2 acetyl

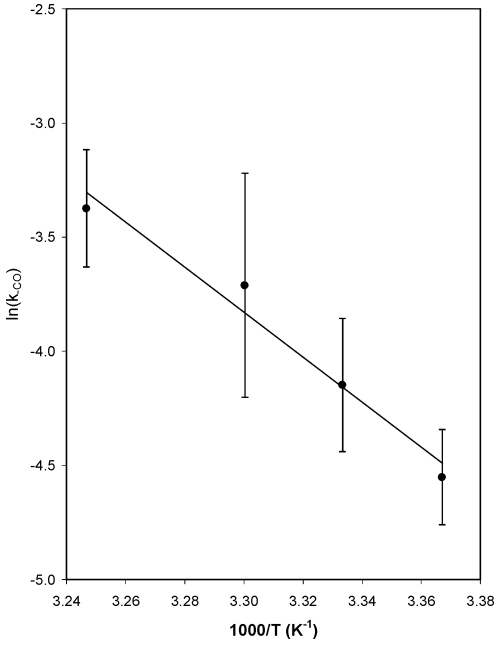

Figure 6. Arrhenius plot for the rate of decarbonylation (k_{-CO}) of species C. Error bars correspond to the standard deviation in k_{-CO} from the intercepts of the plots in Figure 4.

tricarbonyl complex (see Chart 1 for structures). If species A is the adduct, $Fe(CO)_4(C_2H_5I)$, then it would be expected that the observed decay rate (of $\sim$30 s^{-1} at 298 K), whose behavior as a function of CO and C_2H_5I pressure is consistent with a unimolecular process, would involve an oxidative addition process followed by an internal rearrangement to produce either $IFe(CO)_4(C_2H_5)$ or $IFe(CO)_3(\eta^2\text{-}COC_2H_5)$. A rate of $\sim$30 s^{-1} implies that if the rate-limiting step is oxidative addition, then the activation energy is $\sim$16 kcal/mol, assuming a typical preexponential factor of 1×10^{13} s^{-1}. An activation energy of this magnitude is, however, high when it is considered in light of known activation energies for other oxidative addition processes. For example, the addition of dihydrogen to $Fe(CO)_4$ is an oxidative addition processes that has been observed to occur with no or a minimal activation barrier.[36,37] We note that this reaction is quite facile even though it involves a change in spin state on going from $^3Fe(CO)_4 + H_2$ to singlet $H_2Fe(CO)_4$. Similarly, the formation of a π-allyl hydride, $HFe(CO)_3(\eta^3\text{-}C_3H_5)$, from $Fe(CO)_3(\eta^2\text{-}C_3H_6)$ involves both breaking a C−H bond and a change in spin on going from what is thought to be $^3Fe(CO)_3(\eta^2\text{-}C_3H_6)$ to $^1HFe(CO)_3(\eta^3\text{-}C_3H_5)$. Yet, it too takes place with an activation energy that is less than 5 kcal/mol. In both of these situations the overall reaction, as written, is exothermic. Thus, there is precedence for exothermic oxidative addition processes, even those involving a change in spin, taking place with little or no activation energy.

Although in each of the above cases an excited triplet state could be involved as an intermediate along the reaction coordinate, it was not possible to determine that this was the case. However, the collisional deactivation of an excited singlet state of a metal carbonyl to its triplet ground state has been reported to be very facile, with a cross-section that is a good fraction of gas kinetics.[23] Thus, it is highly unlikely that an excited state intermediate of different spin multiplicity than the ground state of the products would be detected under the operative reaction conditions.

Finally, as discussed below, DFT calculations indicate that oxidative addition in this system is exothermic. These observation suggest that species A *is not* $Fe(CO)_4(C_2H_5I)$. Density functional theory calculations support this conclusion. A search for an $Fe(CO)_4(C_2H_5I)$ adduct yielded a minimum energy structure (see Chart 1, structure a) that is $\sim$12 kcal/mol *above* the other possible species: $IFe(CO)_4(C_2H_5)$, $IFe(CO)_3(\eta^2\text{-}COC_2H_5)$, and $IFe(CO)_3(\eta^2\text{-}COC_2H_5)$. Only the *cis* isomer of $IFe(CO)_4(C_2H_5)$ is shown in Chart 1, but as indicated in ref 24, this isomer is expected to be the lower energy isomer. DFT calculations also show that singlet $^1IFe(CO)_4(C_2H_5)$ is significantly lower in energy (by $\sim$44 kcal/mol) than $^3IFe(CO)_4(C_2H_5)$, and thus only $^1IFe(CO)_4(C_2H_5)$ was considered as a stable product. Further, a transition state search between the $Fe(CO)_4(C_2H_5I)$ adduct and $IFe(CO)_4(C_2H_5)$ revealed that the adduct goes to $IFe(CO)_4(C_2H_5)$ without a barrier.

Though conceivably species A could be $IFe(CO)_3(\eta^1\text{-}COC_2H_5)$, this is unlikely because $IFe(CO)_3(\eta^1\text{-}COC_2H_5)$ is an unsaturated 16-electron species. A coordinatively unsaturated complex would not be expected to survive at a detectable concentration for as long as $\sim$30 ms. It would be expected to add CO to form a saturated complex.[20,21] In Section II.A we noted that the decay of species A is, within experimental error, independent of CO pressure. Therefore, the only remaining plausible species that would be expected to be stable at detectable concentrations for $\sim$30 ms or more are the 18-electron species $IFe(CO)_4(C_2H_5)$ and $IFe(CO)_3(\eta^2\text{-}COC_2H_5)$. Recent calculations by Wang and Weitz[24] indicate that $IFe(CO)_4(C_2H_5)$ might be the more thermodynamically stable isomer. Our DFT calculations suggest that $IFe(CO)_4(C_2H_5)$ is the kinetically favored species. Transition state searches from the $Fe(CO)_4(C_2H_5I)$ adduct going to either $IFe(CO)_4(C_2H_5)$ or $IFe(CO)_3(\eta^2\text{-}COC_2H_5)$ yielded a transition state that was geometrically and energetically similar to $IFe(CO)_4(C_2H_5)$ (see Chart 1).

If $IFe(CO)_4(C_2H_5)$ were both kinetically and thermodynamically favored, then this would be the product, or at least the dominant product, observed on the millisecond time scale. If $IFe(CO)_4(C_2H_5)$ is kinetically favored but $IFe(CO)_3(\eta^2\text{-}COC_2H_5)$ is slightly thermodynamically favored, then $IFe(CO)_4(C_2H_5)$ that is initially formed would be expected to convert to $IFe(CO)_3(\eta^2\text{-}COC_2H_5)$. Such a hypothesis, although counter to the energetics of these species as calculated by Wang and Weitz,[24] is still plausible because the enthalpy difference reported in ref 24 favors $IFe(CO)_4(C_2H_5)$ by less than 1 kcal/mol. Such a difference is within the error of the calculations. Given a small enthalpy difference, an equilibrium between A and B would be expected. Species B reaches a maximum at $\sim$75 ms. At that point species A has fallen to $\sim$10% of its maximum level. After this time both species decay. Thus, if equilibrium is reached before significant decay of both species takes place, the free energy difference necessary to account for the

(36) Wang, W.; Narducci, A. A.; House, P. G., Weitz, E. *J. Am. Chem. Soc.* **1996**, *118*, 8654.
(37) Long G. T.; Wang W.; Weitz, E. *J. Am. Chem. Soc.* **1995**, *117*, 12810.

Chart 1

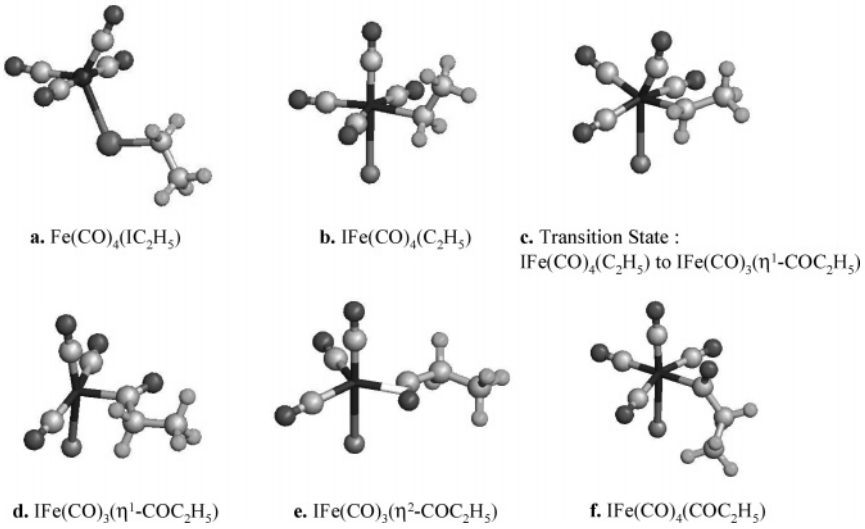

presence of 10% of the initial amount of A at equilibrium is only ~1.3 kcal/mol. Thus, we assign species A as $IFe(CO)_4(C_2H_5)$ and species B as $IFe(CO)_3(\eta^2\text{-}COC_2H_5)$.

Further support for the assignment of species A as $IFe(CO)_4(C_2H_5)$ comes from a comparison of the absorptions of this complex to those of the known $IFe(CO)_4(C_2F_5)$ and $IFe(CO)_4(C_3F_7)$ complexes, which were obtained by Stone and co-workers.[8−10] When the C−O stretching vibrational frequencies of the perfluoroethyl complex (2056, 2087, 2143 cm^{-1}, C_2Cl_4 solution) are compared with those of the ethyl complex in the gas phase (1970, 1998, 2072 cm^{-1}), we note that the frequencies of the corresponding absorptions shift by 70−90 cm^{-1}. The presence of electron-withdrawing fluorine atoms in the alkyl ligand is expected to result in a shift of the CO stretches of the compound to higher frequency.[38] However, the fact that solution phase absorptions are usually lower in frequency than the corresponding gas phase absorption must also be taken into account. In the $Fe(CO)_4(C_2H_4)$ complex this shift is ~10 cm^{-1} for all of the carbonyl stretching modes.[38,39]

It might be anticipated that DFT would be a good predictor of the positions of the carbonyl stretching frequencies of the various complexes of interest in this study. However, as seen in Table 1, we find that agreement between experimental and calculated frequencies (using the same functional and basis set as other calculations in this study) for known iodide complexes is not particularly good. The shifts between calculated and measured frequencies vary sufficiently that these calculations do not provide guidance in making assignments of complexes observed in this study.

In this context, even thought all vibrational modes in a molecule may not shift by the same relative amount on fluorination of a ligand and/or on solvation, the shifts observed between species A and those of the known $IFe(CO)_4(C_2F_5)$ and $IFe(CO)_4(C_3F_7)$ complexes are in sufficiently good agreement that we consider this agreement to be at least consistent with our assignment of species A as $IFe(CO)_4(C_2H_5)$. Table 1 shows the calculated frequencies for these complexes.

The data presented so far, though providing a plausible case that species A is $IFe(CO)_4(C_2H_5)$ and species B is $IFe(CO)_3(\eta^2\text{-}COC_2H_5)$, do not rule out the reverse of these assignments. However, if species A were actually $IFe(CO)_3(\eta^2\text{-}COC_2H_5)$, it is difficult to see how this species could form without a prior oxidative addition step. If this occurred, then $IFe(CO)_4(C_2H_5)$ would be along the reaction pathway to $IFe(CO)_3(\eta^2COC_2H_5)$. Since species B is thermodynamically favored, it would mean that the system accessed the thermodynamically favored species, but equilibrium was not established until after the thermodynamically less favored species was populated to a point beyond its equilibrium concentration. Though this may be possible for a system that is internally excited, prior evidence indicates that internal excitation would not persist on the millisecond time scale for the pressures employed.[20,23] Thus, we feel that the indicated assignments are correct.

In light of these assignments we propose an overall mechanism (Scheme 1) that can explain the kinetic behavior of all the observed products. In this mechanism, photogenerated $Fe(CO)_4$ adds (rate constant k_1) C_2H_5I to form an $Fe(CO)_4(C_2H_5I)$ adduct that undergoes rapid oxidative addition (rate constant k_4) with a very low or no activation energy to yield $IFe(CO)_4(C_2H_5)$ and subsequently $IFe(CO)_3(\eta^2\text{-}COC_2H_5)$ via the unsaturated intermediate, $IFe(CO)_3(\eta^1\text{-}COC_2H_5)$. When sufficient CO is present in the mixture, $IFe(CO)_3(\eta^1\text{-}COC_2H_5)$ adds CO to form $IFe(CO)_4(COC_2H_5)$. $IFe(CO)_4(COC_2H_5)$ decarbonylates slowly, probably via the $IFe(CO)_3(\eta^1\text{-}COC_2H_5)$ intermediate. Either $IFe(CO)_3(\eta^1\text{-}COC_2H_5)$ and/or species it is in equilibrium with then decay to produce unidentified products that accumulate on the walls of the cell. For simplicity, the kinetic model in Scheme 1 contains only one decomposition pathway, which is the pathway for decomposition of $IFe(CO)_3(\eta^1\text{-}COC_2H_5)$, with rate constant k_{dp}.

B. Kinetic and Thermodynamic Analysis. 1. Kinetics of the Decay of $IFe(CO)_4(C_2H_5)$ and $IFe(CO)_3(\eta^2\text{-}COC_2H_5)$. Within experimental error, the decay of both $IFe(CO)_4(C_2H_5)$ and $IFe(CO)_3(\eta^2\text{-}COC_2H_5)$ are independent of CO and C_2H_5I pressures. Further-

(38) House, P. G.; Weitz, E. *J. Phys. Chem.* **1997**, *101*, 2988,
(39) (a) Andrews, D. C.; Davidson, G. *J. Organomet. Chem.* **1972**, *35*, 161. (b) Murdoch, H. S.; Weiss, E. *Helv. Chim. Acta* **1963**, *46*, 1588.

Scheme 1

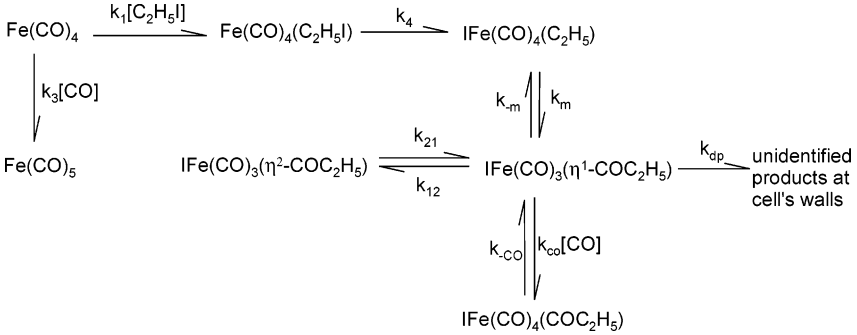

more, temperature dependences for the decay of these products are modest with small activation energies and preexponentials. The magnitude of these preexponentials indicates that the decay of both $IFe(CO)_4(C_2H_5)$ and $IFe(CO)_3(\eta^2\text{-}COC_2H_5)$ are not due to a single elementary reactions, but rather they are phenomenological rate constants resulting from a combination of more than one kinetic process.

To explain experimental observations, a kinetic analysis based on the proposed mechanism (Scheme 1) has been performed using both the steady state approximation for the 16-electron intermediate, $(IFe(CO)_3(\eta^1\text{-}COC_2H_5))$, and stochastic chemical kinetic simulations.[40] When the steady state approximation is applied to $IFe(CO)_3(\eta^1\text{-}COC_2H_5)$, the phenomenological rate constant for decay of $IFe(CO)_4(C_2H_5)$ (product A) is given by

$$k_{\text{obs}}^{\text{A}} = \frac{k_{\text{m}}(k_{12} + k_{\text{co}}[\text{CO}] + k_{\text{dp}})}{k_{12} + k_{-\text{m}} + k_{\text{co}}[\text{CO}] + k_{\text{dp}}} \qquad (9)$$

Note that if addition of CO to $IFe(CO)_3(\eta^1\text{-}COC_2H_5)$ were much faster than any other process, then $k_{\text{obs}}^{\text{A}}$ would effectively be equal to k_{m}. This would imply that the large majority of the $Fe(CO)_4(C_2H_5I)$ would be converted to $IFe(CO)_4(COC_2H_5)$ upon addition of CO and therefore $IFe(CO)_3(\eta^2\text{-}COC_2H_5)$ would not be readily observable. The fact that $IFe(CO)_3(\eta^2\text{-}COC_2H_5)$ is observed implies that the addition of CO to $IFe(CO)_3(\eta^1\text{-}COC_2H_5)$ is not much faster than competing processes, and it is therefore unlikely that $k_{\text{CO}}[\text{CO}] \gg k_{\text{dp}}$, k_{12}, and $k_{-\text{m}}$ under experimental conditions. The apparent independence of this rate on CO pressure indicates that the overall rate for reaction back to $IFe(CO)_4(C_2H_5)$ ($k_{-\text{m}}$) and acetyl slippage (k_{12}) to form the eta-2 product could be significantly faster than the addition of CO to $IFe(CO)_3(\eta^1\text{-}COC_2H_5)$ ($k_{\text{CO}}[\text{CO}]$) and reactions leading to decay of $IFe(CO)_3(\eta^1\text{-}COC_2H_5)$ (k_{dp}). However we note that, as shown in ref 37, the rate for processes involving an intermediate present at low concentration, such as CO addition to $IFe(CO)_3(\eta^1\text{-}COC_2H_5)$, can have a small overall rate since, when such a species is present at a low concentration, the rate of its decay is determined by the product of the rate constant times the appropriately weighted equilibrium (or steady state) concentration.

Similarly, it can be shown that the "phenomenological" rate constant for decay of $IFe(CO)_3(\eta^2\text{-}COC_2H_5)$ is given by

$$k_{\text{obs}}^{\text{B}} = \frac{k_{21}(k_{-\text{m}} + k_{\text{co}}[\text{CO}] + k_{\text{dp}})}{k_{-\text{m}} + k_{12} + k_{\text{co}}[\text{CO}] + k_{\text{dp}}} \qquad (10)$$

From eqs 9 and 10 it is clear that the temperature dependence of the decays of $IFe(CO)_3(\eta^2\text{-}COC_2H_5)$ and $IFe(CO)_4(COC_2H_5)$ is not characteristic of an elementary process, but instead is a manifestation of a combination of various kinetic processes that are involved in the indicated decomposition channel. Chemical kinetic simulations based on Scheme 1 agree with this observation. For simulations at 298 K, the following values (rate constants as indicated in Scheme 1) were fixed: $k_1 = 3 \times 10^9\ \text{M}^{-1}\ \text{s}^{-1}$, $k_3 = 3 \times 10^7\ \text{M}^{-1}\ \text{s}^{-1}$, $k_4 = 1 \times 10^{13}\ \text{s}^{-1}$, and $k_{-\text{CO}} = 0.010\ \text{s}^{-1}$. k_1, k_3, and $k_{-\text{CO}}$ have been experimentally determined, while k_4 is taken to be $1 \times 10^{13}\ \text{s}^{-1}$ based on the prior observation that thermodynamically favored oxidative addition processes involving unsaturated metal carbonyls often have little or no activation energy. All other rate constants were systematically varied in order to obtain the best possible fit to the experimental observations. Equations 9 and 10 were used to obtain initial guesses of the rate constants that reasonably reproduce the observed temperature dependences. As a result of iterating the values of the individual rate constants, the "best fit" set of parameters was as follows: $k_{\text{m}} = 290\ \text{s}^{-1}$, $k_{-\text{m}} = 2.7 \times 10^9\ \text{s}^{-1}$, $k_{12} = 1.2 \times 10^8\ \text{s}^{-1}$, $k_{21} = 15\ \text{s}^{-1}$, $k_{\text{CO}} = 3.0 \times 10^{10}\ \text{M}^{-1}\ \text{s}^{-1}$, $k_{\text{dp}} = 5.0 \times 10^7\ \text{s}^{-1}$. Figure 2 shows the results of the simulations. Note that the rate constants obtained from the simulations indicate that certain terms, such as $k_{\text{CO}}[\text{CO}]$ and k_{dp}, cannot be neglected in the numerator and the denominator of eqs 9 and 10. Thus, the Arrhenius parameters for both $IFe(CO)_4(C_2H_5)$ and $IFe(CO)_3(\eta^2\text{-}COC_2H_5)$ effectively have contributions from the various processes involved in the reactions of the relevant complexes. The simulations indicate that the decay of $IFe(CO)_4(C_2H_5)$ should have a modest linear dependence on the CO pressure, while the dependence on CO pressure of the rate of decay of $IFe(CO)_3(\eta^2\text{-}COC_2H_5)$ should be negligible. For example, according to the simulations, the decay rate of $IFe(CO)_4(C_2H_5)$ should increase ~1.3 times when the CO pressure is doubled. As previously discussed, experimental confirmation of such a dependence was difficult given the limited signal-to-noise levels of the decay signals on longer time scales.

In the case of the formation of the eta-1 intermediate a small preexponetial is the a priori expectation since this reaction is likely to involve a constrained cyclic

(40) *40. Chemical Kinetics Simulations*, Version 1.0.1 for Windows; IBM Research Corp.: Armonk, NY.

transition state. A DFT calculation of the transition state for the formation of $IFe(CO)_3(\eta^1\text{-}COC_2H_5)$ from $IFe(CO)_4(C_2H_5)$ supports this hypothesis as well as the concept that a process of this type involves migration of an ethyl rather than a carbonyl ligand.[16−18,41] As can be seen in Chart 1 (structure c), the transition state (TS) for this process has a cyclic structure. The carbonyl ligand cis to the ethyl group bends toward it, facilitating ethyl migration. In the formation of this transition state the following geometrical changes occurs: the I−Fe−CO angle goes from 179° in $IFe(CO)_4(C_2H_5)$ to 153° with the $OC-C_2H_5$ distance going from 2.85 Å to 1.90 Å and the $OC-Fe-C_2H_5$ angle decreasing from 92° to 54°. The $I-Fe-C_2H_5$ angle goes from 87° in $IFe(CO)_4(C_2H_5)$ to 99° in the TS and the eta-1 intermediate. Furthermore the $Fe-C_2H_5$ bond elongates from 2.19 Å in $IFe(CO)_4(C_2H_5)$ to 2.30 Å in the transition state, but the Fe−CO bond length (1.76 Å) does not change. The calculated activation energy for the process is 8.4 kcal/mol. Using this value, and a rate constant (k_m) of 300 s^{-1} at 298 K, the preexponential factor for this reaction would be about 4×10^8 s^{-1}, which is very small for a gas phase elementary reaction. However, the calculated activation energy does not include zero-point energy or the thermal corrections. Additionally, DFT calculations of activation barriers can have significant errors. Nevertheless, the results all suggest that a small preexponential for such a process is highly likely. Similarly, although the decay of $IFe(CO)_3(\eta^2\text{-}COC_2H_5)$ is a convolution of elementary steps, it may be inferred that the small preexponential factor might be influenced by the presence of a tight transition state as the acetyl slips from the eta-2 to the eta-1 structure.

2. Formation and Decay of $IFe(CO)_4(COC_2H_5)$. The addition of CO to $IFe(CO)_3(\eta^1\text{-}COC_2H_5)$ is a relatively slow side reaction. Because $IFe(CO)_3(\eta^1\text{-}COC_2H_5)$ is an unsaturated 16-electron complex, it is expected to be a steady state intermediate coupled to both $IFe(CO)_3(\eta^2\text{-}COC_2H_5)$ and $IFe(CO)_4(C_2H_5)$. Thus, it is expected to be present in significantly lower concentration than either of the latter two complexes. As discussed in ref 37, the observed rate for a process involving a species in equilibrium (or at steady state) is dependent on the rate constant for the process as well as the relative concentration of that species compared to the overall concentration of the species in the equilibrium. The kinetics simulations confirm this situation.

Consistent with the formation of $IFe(CO)_4(COC_2H_5)$ being a relatively slow process under experimental conditions, more than ~35 Torr of CO are required to produce enough $IFe(CO)_4(COC_2H_5)$ for it to be detected above the noise level of the FTIR spectrometer. However, the kinetics of formation of $IFe(CO)_4(COC_2H_5)$ could not be followed due to the limited signal-to-noise levels that could be obtained on the time scale over which formation of this product occurs (>100 ms). $IFe(CO)_4(COC_2H_5)$ lives for minutes before it decays via decarbonylation, leading to unidentified final products that accumulate on the walls of the cell. Increasing the pressure of CO (up to 250 Torr) increases the concentration of $IFe(CO)_4(COC_2H_5)$ and leads to a *slower* decay rate. The kinetic simulations confirmed such behavior. An activation energy of ~20 kcal/mol and a preexponential of $\sim 3 \times 10^{12}$ s^{-1} were measured for this process. This suggests that decarbonylation occurs via a dissociative mechanism that does not involve a tight transition state.

VI. Conclusions

UV photolysis of $Fe(CO)_5$ in the presence of CO and C_2H_5I generates three novel compounds that have been detected using time-resolved infrared spectroscopy. The assignments for these products have been made based on experimental results in conjunction with DFT calculations,[24] kinetic simulations, and results obtained by other groups.[11−18] The three products are assigned as $IFe(CO)_4(C_2H_5)$, $IFe(CO)_3(\eta^2\text{-}COC_2H_5)$, and $IFe(CO)_4(COC_2H_5)$. A reaction mechanism consistent with experimental observations has been proposed and is shown in Scheme 1. C_2H_5I oxidatively adds to $Fe(CO)_4$ with a rate constant of $\sim 3 \times 10^9$ M^{-1} s^{-1}, producing the oxidative addition product, $IFe(CO)_4(C_2H_5)$. This alkyl iodide complex survives for more than 30 ms, undergoing reaction to form an $IFe(CO)_3(\eta^1\text{-}COC_2H_5)$ intermediate. This complex in turn undergoes (1) acetyl "slippage" to produce the η^2-complex $IFe(CO)_3(\eta^2\text{-}COC_2H_5)$; (2) addition of CO to produce $IFe(CO)_4(COC_2H_5)$, and (3) decay to unidentified products that accumulate on the walls of the cell. The alkyl iodide complex is the kinetically preferred product and converts to the thermodynamically more favorable η^2 product. These experiments also indicate that in the presence of sufficient CO (>35 Torr under experimental conditions) there is another observable product: $IFe(CO)_4(COC_2H_5)$ that results from CO addition to $IFe(CO)_4(C_2H_5)$ and $IFe(CO)_3(\eta^2\text{-}COC_2H_5)$, which is believed to occur via the $IFe(CO)_3(\eta^1\text{-}COC_2H_5)$ intermediate. $IFe(CO)_4(COC_2H_5)$ is stable enough to survive for minutes, decaying slowly via decarbonylation with an activation energy of ~20 kcal/mol and with a preexponetial factor of 3×10^{12} s^{-1}.

Acknowledgment. We acknowledge the support of this work by the National Science Foundation under grant NSF 97-34891.

OM0492348

(41) Becke, A. D.; Hoffmann, R. *J. Am. Chem. Soc.* **1978**, *100*, 7224.